The EMBO Journal Vol.18 No.18 pp.4903–4914, 1999

Cellular retinol-binding protein I is essential for vitamin A homeostasis

Norbert B.Ghyselinck, Claes Båvik[1], Vincent Sapin[2], Manuel Mark, Dominique Bonnier, Colette Hindelang, Andrée Dierich, Charlotte B.Nilsson[3], Helen Håkansson[3], Patrick Sauvant[4], Véronique Azaïs-Braesco[4], Maria Frasson[5], Serge Picaud[5] and Pierre Chambon[6]

Institut de Génétique et de Biologie Moléculaire et Cellulaire, CNRS/INSERM/ULP, Collège de France, 67404 Illkirch Cedex, [4]INRA, Centre de Recherches en Nutrition Humaine, Equipe Vitamines, Clermont-Ferrand, [5]Laboratoire de Physiopathologie Rétinienne, INSERM/ULP, Hôpital Civil de Strasbourg, France and [3]Institute of Environmental Medicine, Karolinska Institutet, Stockholm, Sweden

[1]Present address: Department of Human Ecology, University of Texas, Austin, TX 78812, USA
[2]Present address: INSERM U384 UFR de Médecine et de Pharmacie, BP 38, 63001 Clermont-Ferrand Cedex, France

[6]Corresponding author
e-mail: igbmc@igbmc.u-strasbg.fr

C.Båvik and V.Sapin contributed equally to this work

The gene encoding cellular retinol (ROL, vitA)-binding protein type I (CRBPI) has been inactivated. Mutant mice fed a vitA-enriched diet are healthy and fertile. They do not present any of the congenital abnormalities related to retinoic acid (RA) deficiency, indicating that CRBPI is not indispensable for RA synthesis. However, CRBPI deficiency results in an ~50% reduction of retinyl ester (RE) accumulation in hepatic stellate cells. This reduction is due to a decreased synthesis and a 6-fold faster turnover, which are not related to changes in the levels of RE metabolizing enzymes, but probably reflect an impaired delivery of ROL to lecithin:retinol acyltransferase. CRBPI-null mice fed a vitA-deficient diet for 5 months fully exhaust their RE stores. Thus, CRBPI is indispensable for efficient RE synthesis and storage, and its absence results in a waste of ROL that is asymptomatic in vitA-sufficient animals, but leads to a severe syndrome of vitA deficiency in animals fed a vitA-deficient diet.

Keywords: binding protein/knock-out/post-natal vitamin A deficiency syndrome/retinol/stellate cell

Introduction

Retinol (ROL), or vitamin A (vitA), is indispensable for embryonic development, growth, vision and survival of vertebrates (Blomhoff *et al.*, 1991). With the exception of vision, retinoic acid (RA) has been shown to be the active vitA derivative, whose pleiotropic effects are transduced by two families of nuclear receptors, the RARs and the RXRs (Chambon, 1996). In the cytoplasm, ROL and RA are bound to cellular retinol-binding proteins (CRBP type I and II) and to cellular retinoic acid-binding proteins (CRABP type I and II), that are highly conserved in mammals (Ong, 1994) and belong to a family of cytosolic proteins binding small hydrophobic ligands (Newcomer, 1995). During development, CRBPI is specifically expressed in several tissues including motor neurons, spinal cord, lung, liver (Dollé *et al.*, 1990; Maden *et al.*, 1990; Ruberte *et al.*, 1991; Gustafson *et al.*, 1993) and placenta (Johansson *et al.*, 1997; Sapin *et al.*, 1997). In adults, CRBPI is highly expressed in liver, kidney, lung (Eriksson *et al.*, 1984), brain (Zetterström *et al.*, 1994), retinal pigment epithelium (de Leeuw *et al.*, 1990) and genital tract (Kato *et al.*, 1985; Porter *et al.*, 1985; Wardlaw *et al.*, 1997). In contrast, CRBPII expression is restricted to the yolk sac between embryonic day post-coitum (E)10.5 and E15.5 (Sapin *et al.*, 1997; our unpublished data), the liver at the end of gestation and the small intestine throughout life (Levin *et al.*, 1987; Schaefer *et al.*, 1989).

Numerous studies *in vitro* using purified proteins and/or cell extracts have suggested that CRBPI and CRBPII could play important roles in ROL metabolism, being involved in esterification of ROL with long-chain fatty acids (Ong *et al.*, 1988; Yost *et al.*, 1988; Herr and Ong, 1992), oxidation of ROL to retinaldehyde (RAL; Ottonello *et al.*, 1993; Boerman and Napoli, 1996) and hydrolysis of retinyl esters (RE) into ROL (Boerman and Napoli, 1991). However, the physiological functions of CRBPs are unclear (Troen *et al.*, 1996). To investigate the actual role of CRBPI during mammalian development and post-natal life, we have knocked out the CRBPI gene. Mutant mice are healthy and fertile when fed a vitA-enriched diet. However, CRBPI deficiency results in a marked reduction of liver retinyl palmitate (RP, the main ester of vitA) levels, due to a decreased synthesis from ROL and a faster turnover rate. Accordingly, CRBPI-null mice reared on a vitA-deficient (VAD) diet fully exhaust their RE stores within 5 months, and develop abnormalities characteristic of post-natal hypovitaminosis A (HVA).

Results

Disruption of the CRBPI gene

Mapping and sequencing of genomic clones revealed that the mouse CRBPI gene organization is very similar to that of its human homologue (data not shown; Nilsson *et al.*, 1988). The structure of the targeting vector in which a neomycin (NEO) cassette was inserted into exon E2 is depicted in Figure 1A. One out of 157 G418-resistant clones (QK10) was shown to exhibit the Southern blot pattern expected for a single homologous recombination event (Figure 1B). It was injected into C57BL/6 blastocysts

© European Molecular Biology Organization

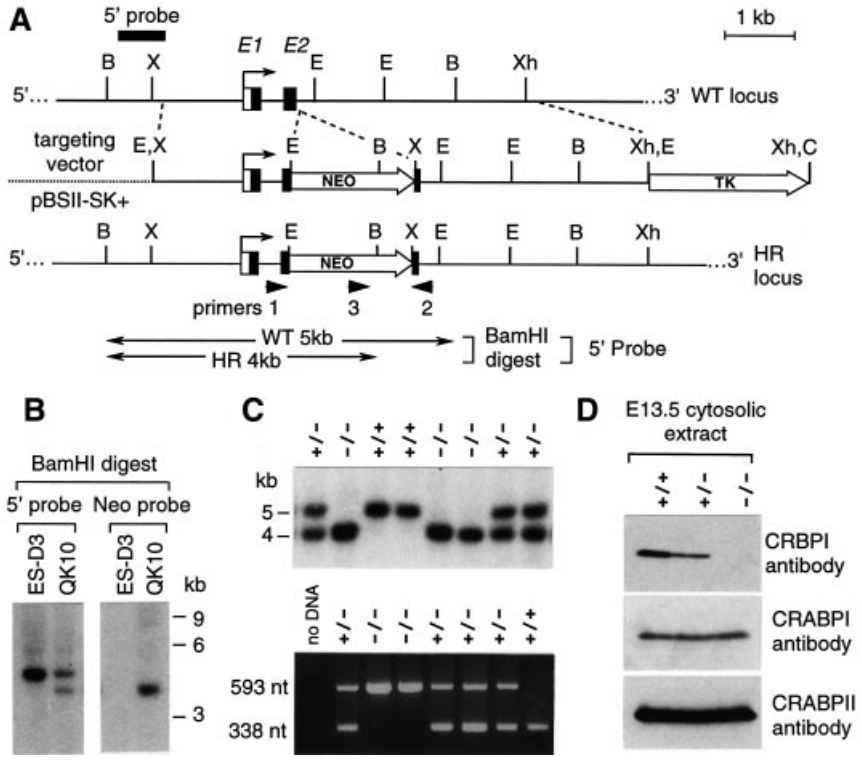

Fig. 1. Disruption of the CRBPI gene. (**A**) Schematic representation of the mouse CRBPI locus. Exons are represented as solid boxes and the promoter as a broken arrow. Structures of the targeting vector and recombinant allele are shown. Primers for PCR genotyping are indicated by arrowheads. Genomic fragments obtained after *Bam*HI digest are indicated for WT and recombinant (HR) alleles. Restriction sites: B, *Bam*HI; C, *Cla*I; E, *Eco*RI; X, *Xba*I; Xh, *Xho*I. (**B**) Genomic DNA from D3 and targeted ES cells (QK10) were analyzed with 5′ external and neomycin probes (A). Size is indicated in kb. (**C**) Southern blot (*Bam*HI digest, upper panel) and PCR analyses (lower panel) of DNA from offspring of a CRBPI$^{+/-}$ intercross. (**D**) Western blot analysis of 40 μg of cytosolic extracts from E13.5 WT (+/+), heterozygous (+/–) and homozygous (–/–) fetuses using a CRBPI-specific antiserum. Note the absence of CRBPI in mutant embryos. After stripping, the blot was reprobed with CRABPI and CRABPII antisera.

to create chimeric mice, of which two males transmitted the mutation to their offspring (see Figure 1C).

To check that CRBPI gene disruption was efficient, mRNA (data not shown) and protein expression were analyzed. Antibodies directed against CRBPI detected the protein (~16 kDa) in extracts from E13.5 wild-type (WT) and heterozygous fetuses, but not in homozygous mutants (Figure 1D), whereas CRABPI and CRABPII expression were not modified. We conclude that the present CRBPI gene disruption is a null mutation.

CRBPI-null mice appear essentially normal

Heterozygous matings ($n = 35$) yielded 24.8% ($n = 72$) of WT, 50% ($n = 145$) of heterozygous and 25.2% ($n = 73$) of homozygous mice, which corresponds to the Mendelian ratio. Male and female mutant mice fed a vitA-enriched diet grew normally, were fertile, healthy up to 20 months of age and indistinguishable from WT littermates. Serial sections of E14.5, E16.5 and E18.5 mutant fetuses ($n = 3$), placentas ($n = 3$) and adult eyes ($n = 5$) did not reveal any histological abnormality, and whole-mount skeletal analysis of CRBPI-null newborns ($n = 20$) did not reveal any malformation. Thus, despite the specific expression pattern of CRBPI in embryonic and adult tissues (see Introduction), mutant mice fed a vitA-enriched diet did not show any abnormality, either during development or after birth. As this lack of obvious defects might reflect a functional compensation of CRBPI by CRBPII, the expression of the latter was investigated.

From E8.5 to E18.5, the expression pattern of CRBPII transcripts analyzed using *in situ* hybridization was identical in WT and CRBPI-null embryos, fetuses and placentas (data not shown; see Dollé *et al.*, 1990; Ruberte *et al.*, 1991; Sapin *et al.*, 1997). At E18.5 and at birth, CRBPII mRNA was co-expressed with CRBPI in liver (Figure 2D), in which the CRBPII protein was confined to hepatocytes (Figure 2C), while the CRBPI protein was detected mainly in cells lining liver blood vessels (Figure 2A). The level of CRBPII mRNA was 2-fold higher in CRBPI-null liver than in WT liver (Figure 2D). The reason for this increase is unclear. It might be due to a higher local production of RA, as (i) CRBPII expression is known to be inducible by RA (Nakshatri and Chambon, 1994), and (ii) the expression level of the RA-inducible RARβ2 gene (Sucov *et al.*, 1990) was also increased in the liver of newborn and 2-week-old CRBPI-null mice (Figure 2D). CRBPII mRNA was not detected in liver at any other fetal or postnatal stage (Figure 2D), nor in any other tissue known to express CRBPI (see Introduction; data not shown). Thus, with the possible exceptions of the yolk sac between E10.5 and E15.5 and of the liver during the neonatal period, it is unlikely that the apparent dispensability of CRBPI during development could correspond to a functional redundancy with CRBPII.

Retinyl ester stores are decreased in liver of CRBPI-null mice

We analyzed ROL homeostasis in liver, which expresses high levels of CRBPI and metabolizes and stores ROL.

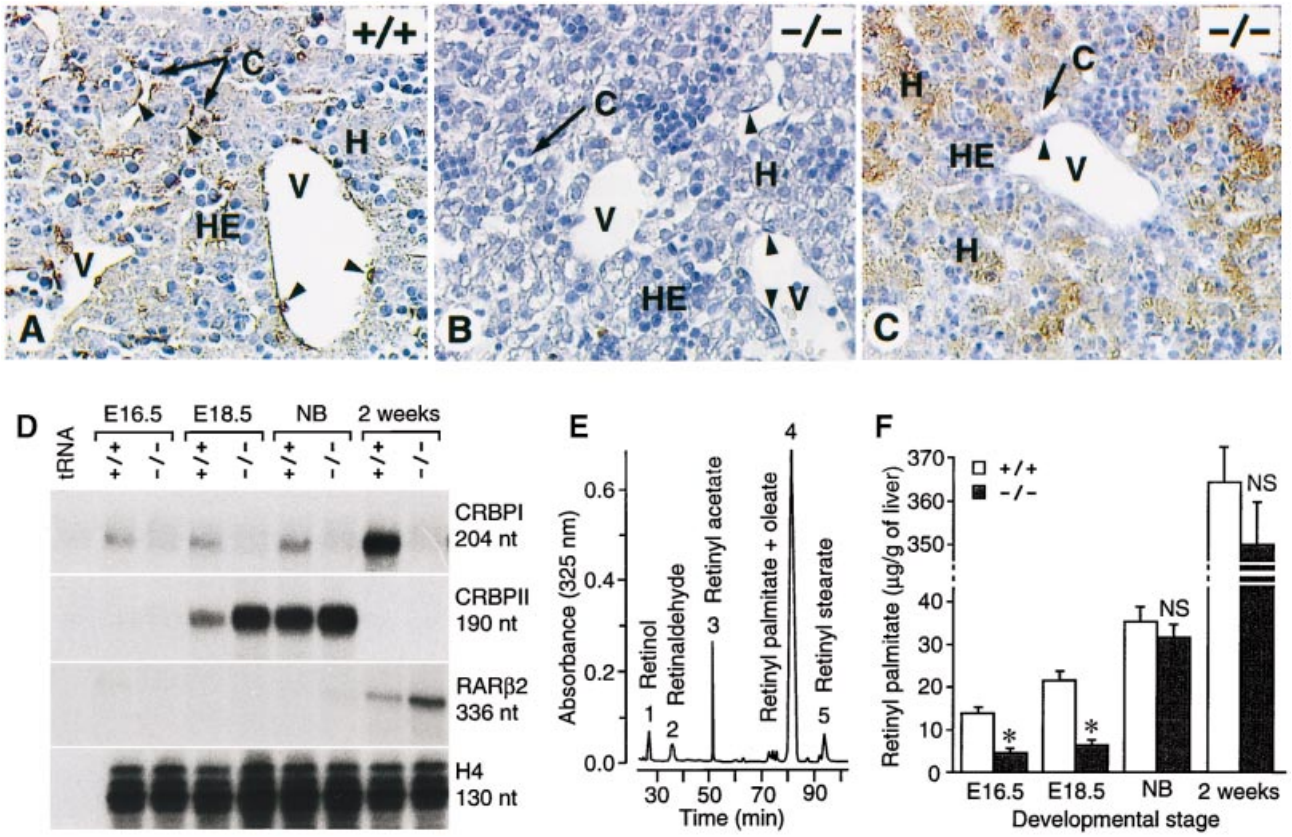

Fig. 2. CRBPII may compensate for the lack of CRBPI in the liver during the neonatal period. (A–C) Immunohistochemical localization of CRBPI and CRBPII in WT (+/+) and CRBPI-null (–/–) liver at 1 day of age. (**A**) CRBPI is expressed in sinusoid lining cells (arrowheads) and hepatocytes, albeit at very different levels. (**B**) Lack of immunostaining with anti-CRBPI antibody in the CRBPI-null liver. (**C**) CRBPII expression is restricted to hepatocytes. The immunostaining pattern is identical in WT liver (not illustrated). C, capillaries (liver sinusoids); H, hepatocytes; HE, hematopoietic cells; V, venules. Arrowheads point to endothelial cells. Magnifications ×400. (**D**) RNase protection assays using 50 μg of total RNA extracted from livers. A tRNA sample was used as background control. Note that signals obtained with the CRBPI probe in CRBPI-null samples corresponded to background. (**E**) Example of an HPLC analysis of retinoids extracted from adult mouse liver. Peaks 1–5 have retention times corresponding to ROL (1), RAL (2), retinyl acetate (3, internal standard), retinyl palmitate (RP) + retinyl oleate (4) and retinyl stearate (RS; 5), respectively. Note that RP and retinyl oleate have identical retention times, but the latter is a minor RE component in liver. RP and RS represented 90 and 10% of mouse liver RE, respectively. The RP/RS ratio was always the same in CRBPI-null and WT livers. (**F**) RP concentrations in livers of +/+ (white bars) and –/– (black bars) E16.5 and E18.5 fetuses, newborn (NB) and 2-week-old mice. An asterisk indicates a significant difference with WT values ($P < 0.05$). NS, not statistically significant.

Table I. Accumulation of retinaldehyde (μg/g of tissue) in liver, kidney and lung of WT (+/+) and CRBPI-null (–/–) mice

		CRBPI genotype	
Tissue	Age (weeks)	+/+	–/–
Liver	6	0.24 ± 0.05	0.19 ± 0.04
Lung	2	1.44 ± 0.15	1.08 ± 0.25
	6	1.42 ± 0.21	1.07 ± 0.20[a]
Kidney	2	0.98 ± 0.13	0.71 ± 0.07
	6	0.46 ± 0.04	0.26 ± 0.02[a]

Data (μg/g of tissue) shown represent mean ± SEM values for 10–15 samples per data point.
[a]Significantly different from the WT value ($P < 0.05$).

Endogenous retinoids were quantified by HPLC (Figure 2E). Oxidation of ROL did not appear to be modified in adult CRBPI-null mice, as their hepatic RAL concentration was not significantly different from that of WT mice (Table I). Retinyl palmitate (RP), which represented 90% of RE (Figure 2E), was detected in liver of E16.5 WT fetuses and its level increased in E18.5 fetuses and suckling newborns (Figure 2F). RP was also found in the liver of CRBPI-null fetuses (E16.5 and E18.5), indicating that mutants can take up and store vitA. However, RP levels were 3-fold lower than in WT fetuses ($P < 0.05$; Figure 2F). In contrast, at post-natal day 1 and at 2 weeks of age, the content of RE in liver of suckling mutants was not different from that of their WT littermates. At these stages, similarly low levels of ROL were detected in liver of WT and CRBPI-null mutants (data not shown). From 4 weeks of age, the amount of liver RP (Figure 3A) and ROL (not shown) were ~50% lower in CRBPI-null mice than in WT animals. After weaning, a slight decrease of RP accumulation was observed (Figure 3A, inset). This probably reflects the nutritional modification from maternal milk to diet pellets.

In mammals, ROL is stored as large cytoplasmic lipid droplets composed of RE in hepatic stellate cells (HSC) located within the interstitial space between hepatocytes and endothelial cells (Wake, 1980; Blomhoff *et al.*, 1991). HSC contain high levels of CRBPI and enzymes esterifying ROL (Blaner *et al.*, 1985; Blomhoff *et al.*, 1985). Light microscopy showed that HSC of CRBPI-null mice contained less abundant and smaller lipid droplets than their WT counterparts (Figure 3B). However, the CRBPI-

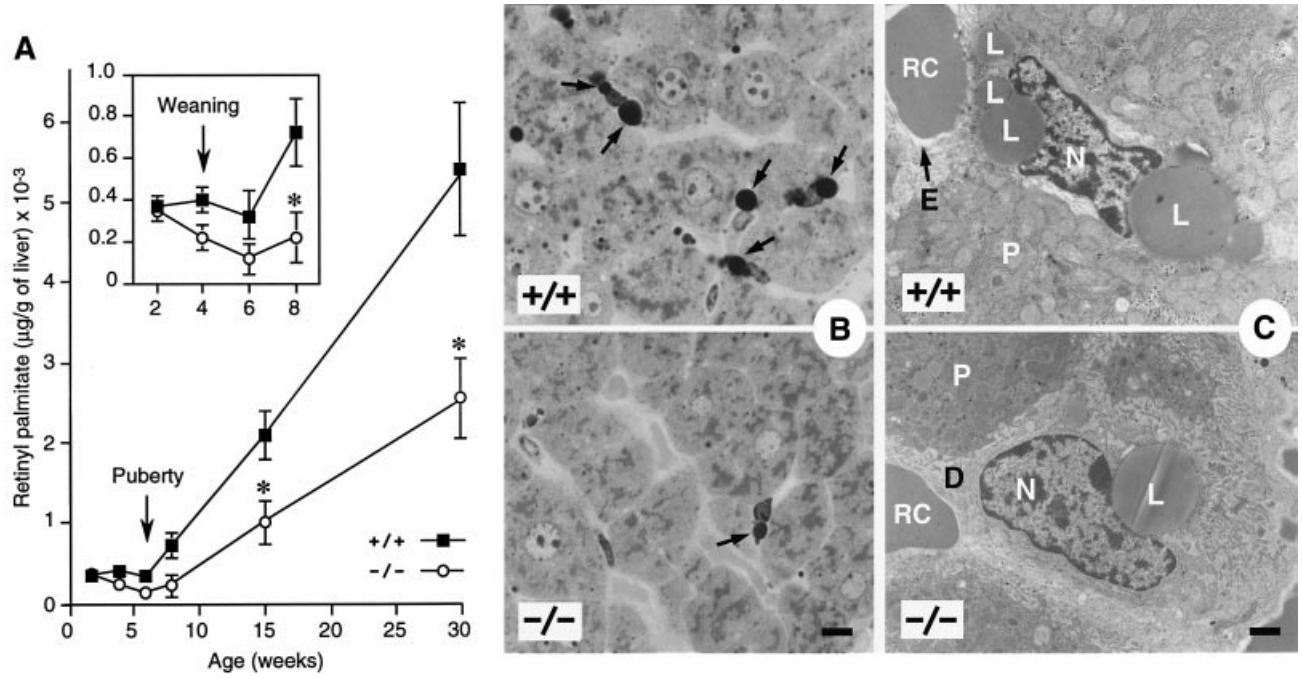

Fig. 3. Hepatic accumulation of retinyl palmitate and histology of stellate cells. (**A**) Mean RP concentrations in liver of WT (+/+, filled squares) and CRBPI-null (–/–, open circles) mice from 2 to 30 weeks of age. Each point represent an average of 8–20 determinations, and vertical bars indicate SEM. Asterisks indicate significant differences from +/+ values ($P < 0.01$). The inset represents an enlargement of the early post-natal period. Note that RP and RS amounts were always 1.5-fold higher in females than in males (not shown). (**B**) Semi-thin sections of 8-week-old male livers stained with toluidine blue. Arrows indicate lipid droplets which are more abundant and bigger in WT than in CRBPI-null hepatic stellate cells (HSC). The bar represents 10 µm. (**C**) Electron microscopy showing that CRBPI-null HSC contained only one or a few small lipid droplets in their cytoplasm. The bar represents 1 µm. D, Disse's space; E, endothelium; L, lipid droplet; N, nucleus of the stellate cell; P, parenchymal cell; RC, red blood cell.

null HSC were ultrastructurally normal (Figure 3C), and immunostaining for vimentin indicated that HSC were as numerous in mutant as in WT liver (data not shown).

Retinol homeostasis in liver of adult CRBPI-null mice

Retinoid homeostasis in liver results from a dynamic balance between storage (re-esterification of ROL originating from blood chylomicrons) and mobilization of stores (hydrolysis of RE in HSC). Esterification of ROL is catalyzed by two enzymes, lecithin:retinol acyltransferase (LRAT) and acyl-CoA:retinol acyltransferase (ARAT). Mobilization of ROL requires retinyl ester hydrolase (REH) activities classified into two classes, according to their dependency upon bile salts: (i) bile-salt-dependent neutral REH (nREH; Cooper and Olson, 1986; Harrison, 1993); and (ii) bile-salt-independent acidic activity (aREH; Mercier *et al.*, 1994). LRAT, ARAT, nREH and aREH whole-liver activities were similar in WT and CRBPI-null mutants (Table II and data not shown).

We next analyzed vitA turnover. A single dose of tritiated ROL was given orally to WT and CRBPI-null mice. Passage of [^{3}H]ROL through the gastrointestinal tract seemed normal in mutants, as the recovery of radioactivity in small intestine 6 h after dosing was similar in WT and CRBPI-null mice (data not shown). The amount of tritium present in liver after 6 h reflects the uptake of radiolabeled chylomicron remnants from blood, but also, and principally the esterification of [^{3}H]ROL originating from them (Blomhoff *et al.*, 1991). In WT liver, 10% of the radioactive dose was taken up after 6 h (Figure 4A), out of which 80% co-eluted with RP, while the remaining 20% co-eluted with ROL (HPLC data not shown). In contrast in CRBPI-null liver, only 5% of the dose was taken up after 6 h, of which 65 and 35% co-eluted with RP and ROL, respectively. Two days later, the [^{3}H]ROL present in the liver no longer reflects uptake and esterification of ROL, but rather the turnover of RE stores (Blomhoff *et al.*, 1991). Their estimated half-life ($t_{1/2}$) was 60 days for WT and 10 days for CRBPI-null mice (Figure 4A), thus indicating a 6-fold shorter turnover time of RE in mutant liver.

We also investigated whether ROL might be degraded faster in the liver of CRBPI-null mutants. Enzymes of the cytochrome P450 (CYP) system play an active role in the oxidative degradation of retinoids (reviewed in Duester, 1996). The mRNA level for CYP26 (Abu-Abed *et al.*,

Table II. Comparison of enzymatic activities in WT (+/+) and CRBPI-null (–/–) adult livers

	CRBPI genotype	
Enzyme activity (pmol/min/mg)	+/+	–/–
LRAT	23 ± 2	25 ± 2
ARAT	1.1 ± 0.1	1.2 ± 0.1
aREH	276 ± 20	255 ± 15
nREH	121 ± 6	105 ± 6
EROD	90 ± 2	114 ± 8[a]
PROD	65 ± 3	71 ± 3[a]

Each value (pmol/min/mg) is the average ± SEM of at least eight individual liver homogenates. Note that ARAT and LRAT activities were 1.5-fold higher in females than in males (not shown).
[a]Significantly different from the WT value ($P < 0.05$).

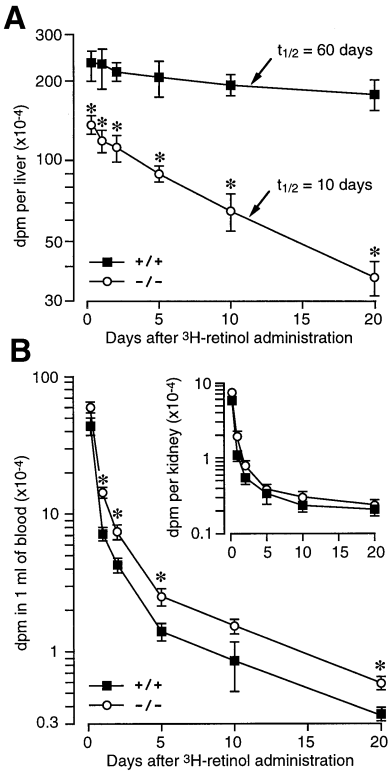

Fig. 4. Turnover of [^{3}H]retinol. WT (+/+) and CRBPI-null (–/–) mice are represented by filled squares and open circles, respectively. Each point represents an average of eight observations, and vertical bars indicate SEM. Asterisks indicate a significant difference from +/+ values ($P < 0.01$). (**A**) The amount of tritium (d.p.m.) in whole liver is plotted on a logarithmic scale against time. Regression lines, calculated between days 2 and 20 after [^{3}H]retinol administration, gave estimated tritium half-lifes ($t_{1/2}$) of 60 days in +/+ and 10 days in –/–. (**B**) The amounts of tritium in blood and in whole kidney (inset) are plotted on a logarithmic scale against time.

1998) was identical in liver of CRBPI-null and WT mice (data not shown). However, CYP1A- and CYP2B-mediated catabolism (estimated by analyzing EROD and PROD activities in whole-liver homogenates) were slightly, but significantly, increased in the liver of CRBPI-null mutants (Table II). We therefore conclude that in the liver of CRBPI-null mice (i) a lower amount of dietary ROL could be taken up, (ii) a lower proportion of newly incoming ROL is esterified as RP, (iii) RE stores have a faster turnover time, and (iv) the degradation of ROL may be slightly increased.

Retinol homeostasis in lung and kidney of CRBPI-null mice

Although 90% of total body vitA is stored in liver, lungs, which express high levels of CRBPI, also store vitA (Shenai and Chytil, 1990). At E16.5, the lung RP content was significantly lower ($P < 0.05$) in CRBPI-null fetuses (14.3 ± 0.7 μg/g of tissue) than in WT (27.6 ± 1.4 μg/g of tissue), but the RP/RS ratio was unchanged (75% RP and 25% RS, see legend to Figure 2E). Only low levels of ROL were detected in fetal lungs, with a ~35% decrease in CRBPI-null mutants when compared with WT (9.4 ± 0.9 μg/g of tissue in mutants versus 14.6 ± 1.4 μg/g of tissue in WT; $P < 0.05$). At later stages, ROL and RP contents were similar in WT and CRBPI-null lungs (data not shown), whereas the RAL level was significantly ($P < 0.05$) decreased by ~25% in adult mutants (Table I).

The kidney is also rich in CRBPI (Eriksson *et al.*, 1984) and is known to play a role in ROL homeostasis (Peterson *et al.*, 1973). At all stages after birth, ROL and RP contents were decreased by ~30% in kidney of CRBPI-null mutants (data not shown). However, whole-kidney esterifying activities were similar (LRAT: 2.87 ± 0.41 versus 2.13 ± 0.53 pmol/min/mg; ARAT: 1.02 ± 0.83 versus 1.88 ± 0.82 pmol/min/mg) in WT and CRBPI-null mutant mice, respectively. The level of RAL was significantly ($P < 0.05$) decreased by ~25% in adult mutants compared with WT (Table I). Finally, both plasma (0.35 μg/ml) and urinary (0.1 μg/ml) ROL concentrations were normal.

We also measured ROL turnover in blood and kidney (Figure 4B). In both cases, following a rapid decrease of [^{3}H]ROL during the first 24 h, a more gradual decline was observed over a period of 20 days. The decay curves for CRBPI-null mutants were similar to those of WT. The observation that [^{3}H]ROL was more abundant in blood and kidney of mutants might reflect a higher rate of depletion from liver stores (see above). It therefore appears that blood clearance and turnover of ROL in kidney are similar in WT and CRBPI-null mice.

Dietary hypovitaminosis A results in a vitA deficiency syndrome in CRBPI-null mice

As the turnover of ROL was faster in mutants, CRBPI deficiency may result in a depletion of ROL stores under conditions of dietary HVA. To investigate this possibility, CRBPI-null and WT mice initially weighing ~16 g were reared from weaning under a VAD diet. Food consumption was not different between WT and mutants (data not shown), and growth was initially used to monitor their retinoid status. WT mice grew steadily during 23 weeks on VAD diet, while CRBPI-null mice grew at a slower rate from the 5th to the 12th week, and then stopped growing during the next 11 weeks (Figure 5A). Every 3 weeks, three to five mice were killed and their liver RP and serum ROL levels were determined. RP levels rapidly decreased in CRBPI-null mutants during the first 14 weeks to become undetectable (Figure 5B, open red circles). In contrast, WT mice still had important RP liver stores, even at 23 weeks (~120 μg/g of liver; Figure 5B, filled red squares). RP half-life was estimated to be 14 days in CRBPI-null mutants versus 84 days in WT. Thus in agreement with RE turnover (Figure 4A), mutant mice exhausted their liver RP stores six times faster than WT littermates. For all mice, ROL serum levels remained stable for 12 weeks (~0.35 μg/ml of serum). When CRBPI-null mutant RP stores dropped below 2 μg/g of liver (14 weeks), ROL serum levels decreased to reach ~0.05 μg/ml at 23 weeks (Figure 5B, open blue circles). In contrast, WT mice maintained a normal serum ROL level during the same period (Figure 5B, filled blue squares). Thus, CRBPI appears to be indispensable for maintaining homeostasis of ROL under conditions of dietary vitA deprivation.

These results prompted us to look for abnormalities characteristic of HVA. The initial change observed in VAD rats is a decline of the electroretinogram (ERG)

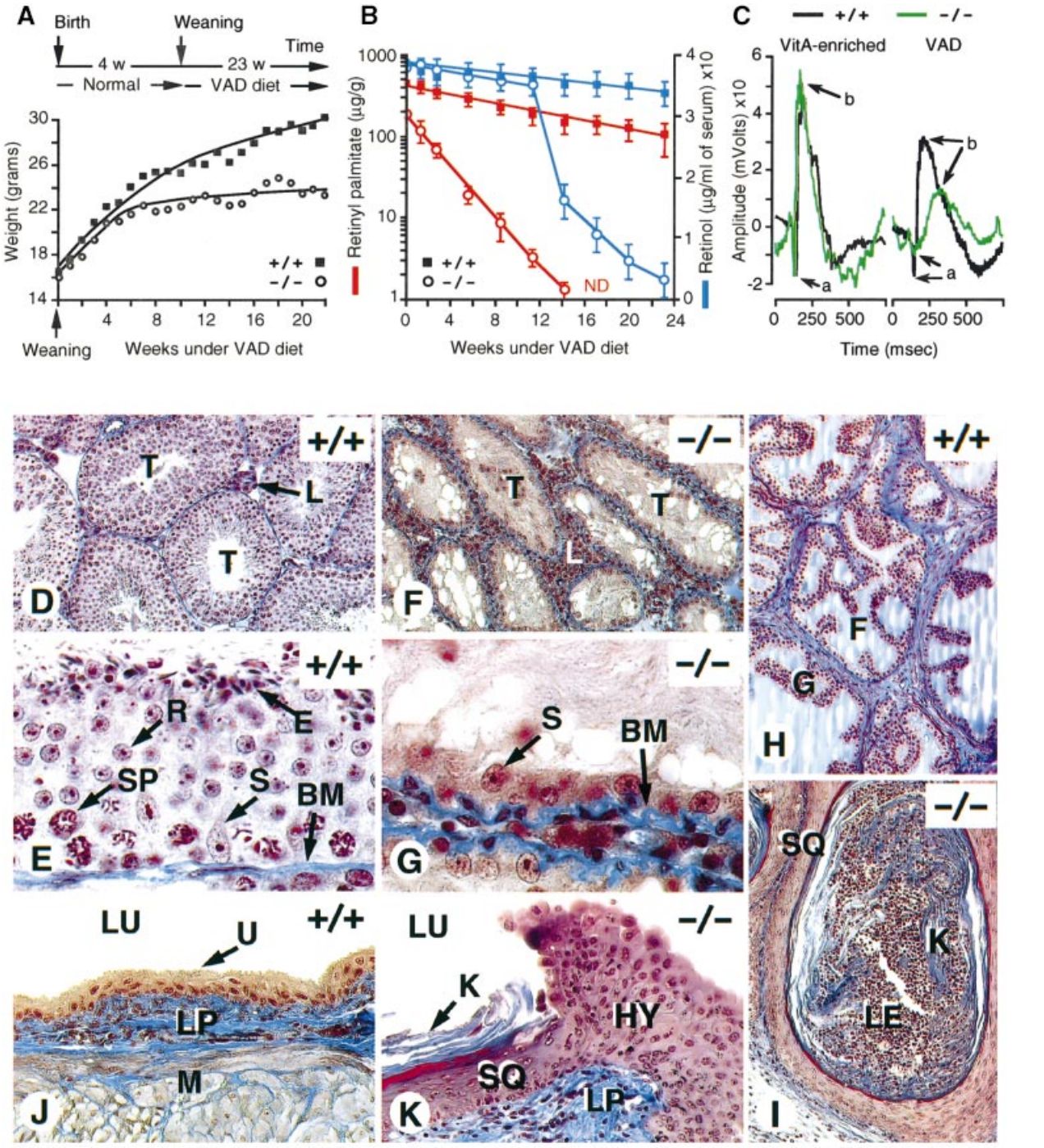

Fig. 5. CRBPI-null mice fed a VAD diet exhaust their RP stores and present symptoms of HVA. (**A**) Schematic representation of the nutritional protocol. Mice were fed a vitA-enriched diet from birth to 4 weeks (w), and then a VAD diet for 23 weeks. The weight of CRBPI-null mice (–/–; open circles) was significantly below that of WT mice (+/+; filled squares) from VAD week 5 onwards ($P < 0.05$). (**B**) Liver RP (red lines) and blood ROL (blue lines) concentrations in WT (+/+; filled squares) and mutant (–/–; open circles) mice, as a function of time. Each point represents the average of three to five observations, and vertical bars indicate SEM. Regression lines calculated between VAD weeks 1 and 14 gave estimated half-lifes ($t_{1/2}$) of 84 days in WT and 14 days in CRBPI-null mutants. ND, not detectable. (**C**) Typical example of dark-adaptated ERG responses from WT (+/+; black line) and mutant (–/–; green line) mice fed the vitA-enriched diet (left panel) or fed the VAD diet for 23 weeks (right panel). a and b denote a- and b-waves, respectively. (D–K) Histological sections through testes (**D**–**G**), cranial prostate (**H** and **I**) and urinary bladder (**J** and **K**) of WT (+/+; D, E, J and H) and CRBPI-null (–/–; F, G, K and I) males maintained on a VAD diet during 23 weeks. All WT tissues were unaffected. In contrast, testes of VAD mutants were degenerated; the glandular epithelium (G) of the cranial prostate, which normally secretes part of the seminal fluid (F), was completely keratinized and the lumen of the gland was filled with both desquamated keratinized cells (K) and leucocytes (LE); the bladder showed foci of squamous metaplasia (SQ) which were often adjacent to hyperplastic areas of the urinary epithelium (HY). BM, basement membrane of the seminiferous tubules; E, elongated spermatids; F, seminal fluid; G, normal (pseudostratified, columnar) prostate glandular epithelium; HY, hyperplastic urinary epithelium; K, desquamated keratinocytes; L, Leydig cells; LE, leucocytes; LP, lamina propria of the urinary bladder; LU, lumen of the bladder; M, smooth muscle cell layers of the bladder; R, round spermatids; S, nuclei of Sertoli cells; SP, spermatocytes; SQ, stratified squamous epithelium; T, seminiferous tubules; U, normal (transitional) epithelium of the bladder. Magnifications: ×100 (D, F, H and I), ×500 (E and G), ×200 (J and K).

Table III. ERG responses of dark-adapted WT (+/+) and CRBPI-null (–/–) mice bred on a vitamin A-enriched (normal) or on a vitamin A-deficient (VAD) diet

		a-wave		b-wave	
Diet	CRBPI genotype	Amplitude (μV ± SD)	Latency (ms ± SD)	Amplitude (μV ± SD)	Latency (ms ± SD)
Normal	+/+	220 ± 46	33 ± 3	764 ± 81	72 ± 9
	–/–	236 ± 30	33 ± 2	623 ± 109	90 ± 12
VAD	+/+	171 ± 15	34 ± 1	488 ± 81	95 ± 8
	–/–	35 ± 17[a]	49 ± 5[a]	240 ± 7[a]	170 ± 47[a]

Amplitudes (μV) and implicit times (latency; ms) are expressed as mean ± SD of three to five animals.
[a]Significantly different from the WT value ($P < 0.01$).

amplitudes (Dowling and Wald, 1958). ERG recordings were normal in both WT and CRBPI-null mutants fed the vitA-enriched diet (Figure 5C and Table III). The VAD diet slightly affected ERG recordings in WT animals (Figure 5C, black recording). In contrast, ERG was dramatically affected in CRBPI-null mutants fed the VAD diet for 23 weeks. Not only were the a- and b-wave amplitudes dramatically decreased (Figure 5C, green recording), but their latency (implicit) times were also increased (Table III). The decrease observed on the first ERG was even more marked upon subsequent ERGs recorded at 3 min intervals (data not shown). Electron microscopic analysis of the eyes showed that the intimate contact made through microvilli between the retinal pigment epithelium (RPE) cells and the outer segment photoreceptors (OS), was disrupted in the CRBPI-null mice fed the VAD diet (compare Figure 6A with B). Furthermore, some of the OS photoreceptors lost their normal shape (asterisks) due to swelling of their lamellar disks that form large vesicles. The highly distorted OS (arrowhead) were mis-oriented, filled with amorphous material and sometimes replaced by lamellar bodies (LB) displaying myelin-like figures. In this context, the transfer of retinoids between RPE and photoreceptors might be less efficient in CRBPI-null mutants than in WT. Similar modifications, which could induce ERG alterations, have been described previously in retinas of VAD rats (Carter-Dawson *et al.*, 1979).

In rat, post-natal HVA affects several tissues including salivary gland, trachea, lung, genital tract and gonads (Wolbach and Howe, 1925; Beaver, 1961). All of these tissues, when collected from WT mice fed the VAD diet for 23 weeks, were histologically normal (Figure 5D, E, H, J, and data not shown). Tissues collected from CRBPI-null mice appeared normal up to the 12th week. At 14 weeks, a testicular degeneration, manifested by the sloughing of immature germ cells (i.e. spermatocytes and round spermatids) in the lumen of seminiferous tubules and the appearance of irregular vacuoles in the epithelium lining the degenerating tubules, was observed in CRBPI-null mutants fed the VAD diet. The lesions were patchy throughout the organ, in which histologically normal seminiferous tubules coexisted with adjacent tubules that had a reduced diameter and/or were mostly devoid of germ cells (not shown). At 23 weeks, the seminiferous tubules of all six mutants analyzed were markedly reduced in size (compare Figure 5D and F), and displayed Sertoli cells only (compare Figure 5E and G). All six mutants also exhibited foci of squamous keratinizing metaplasia of: (i) the pseudostratified columnar epithelia in the prostate (compare Figure 5H and I, and data not shown) and the seminal vesicle (not shown); and (ii) the stratified transitional epithelium in the urinary bladder (compare Figure 5J and K) and the penile urethra (not shown). In addition, four mutants displayed keratinization of the cuboidal epithelium lining the small collecting tubes in the salivary gland (not shown), whereas vas deferens as well as epididymis were occasionally keratinized (one out of six; not shown). Other epithelia known to be highly susceptible to squamous keratinizing metaplasia in VAD rats (e.g. trachea, bronchi) were not affected. Taken collectively, these results indicate that a VAD diet results in a syndrome of post-natal HVA much more readily in CRBPI-null mutants than in WT.

Discussion

Since the discovery of CRBPI 25 years ago (Bashor *et al.*, 1973), its three-dimensional structure, binding properties, tissue localization, regulation of expression and involvement *in vitro* in ROL metabolism have been extensively studied (reviewed in Blomhoff *et al.*, 1991; Ross, 1993; Ong, 1994; Napoli, 1997). While it was assumed that CRBPI could play a major role in vitA homeostasis, its actual physiological role remained unknown. To investigate CRBPI function *in vivo*, we have created a null mutation in the mouse.

Apparent dispensability of CRBPI during development

The conservation of CRBPI in vertebrates and its specific pattern of expression in embryos and fetuses have suggested that it could play important roles in retinoid signaling during development (Dollé *et al.*, 1990; Ruberte *et al.*, 1991). However, no embryonic, fetal or placental alteration could be detected in CRBPI-null mutants, indicating the dispensability of this protein during intra-utero development. However, liver RP stores are lower in CRBPI-null fetuses (E16.5 and E18.5) than in WT littermates. This suggests that CRBPI is required for efficient formation and storage of RE in fetal liver. Alternatively, this may also suggest that transfer of ROL through CRBPI-null placenta may be less efficient than through WT placenta. This possibility is supported by the observation that the uptake of ROL by placental membrane *in vitro* is enhanced in the presence of CRBPI (Sundaram *et al.*, 1998). In any event, our results indicate that CRBPI is dispensable in embryos and fetuses, at least under conditions of maternal vitA dietary excess. Further studies are

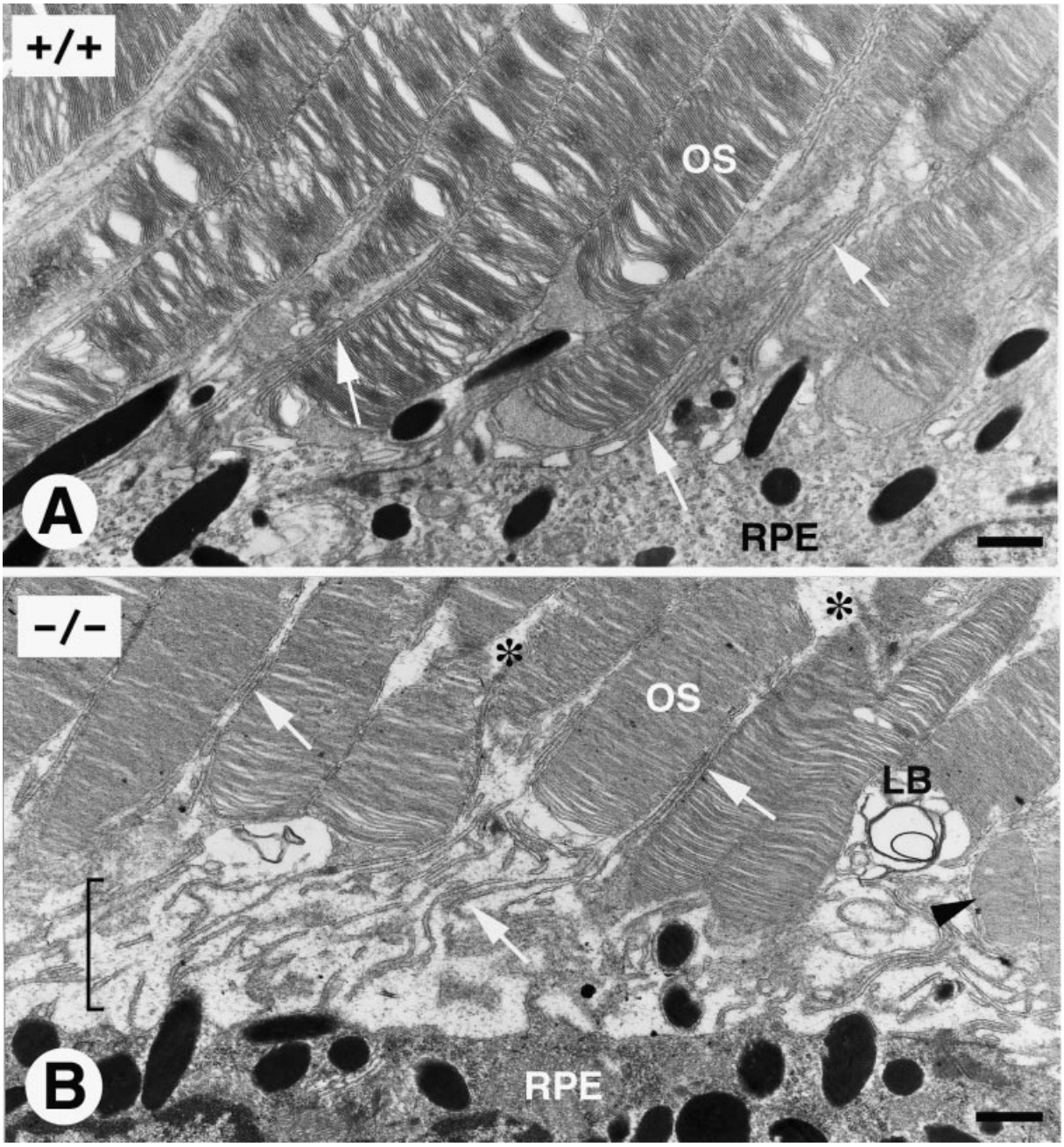

Fig. 6. Electron micrographs of longitudinal sections through retinas of WT and CRBPI-null mice fed a VAD diet for 23 weeks. (**A**) In WT, the OS consisted of stacks of transverse disks, enclosed within the cell membrane. Note that some of them were artefactually distorted by clefts produced during fixation. Numerous microvilli (arrows) are present between the OS which are in close contact with the RPE cells. (**B**) In CRBPI-null eyes, the intimate contact between the RPE and the OS was lost. It was replaced by a large space (brackets) in which some microvilli were lying (arrows). Numerous OS photoreceptors had an abnormal shape (asterisks). The highly distorted OS (arrowhead) were mis-oriented, filled with amorphous material and were sometimes replaced by lamellar bodies displaying myelin-like figures. LB, lamellar bodies; OS, outer segment photoreceptors; RPE, retinal pigment epithelium. Bars represent 0.5 μm.

needed to investigate whether CRBPI is required in fetuses under conditons of maternal vitA deficiency. After birth, ROL is provided by milk. As liver RP contents are identical in mutant and WT newborns, CRBPI appears to be dispensable for ROL hepatic uptake and esterification during the neonatal period. The presence of CRBPII in liver around birth may account for this apparent dispensability of CRBPI, as CRBPII may facilitate RE synthesis (Ong *et al.*, 1988).

CRBPI is important for retinol homeostasis

The capacity to store incoming ROL and to maintain RP stores is impaired in liver of CRBPI-null mice. This cannot be accounted for by a lower intestinal absorption of vitA, as incorporation of [^{3}H]ROL in mutant small intestine does not differ from that in WT. Furthermore, blood RP content (indicative of the presence of chylomicrons) is identical in WT and CRBPI-null mice, suggesting that ROL incorporation into chylomicrons (which is dependent

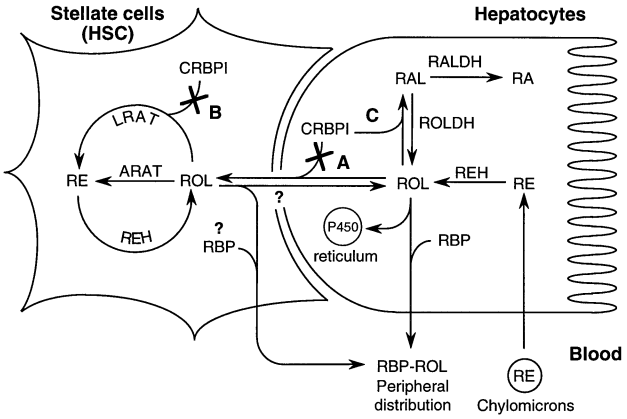

Fig. 7. Hepatic metabolism of ROL. Hepatocytes take up chylomicrons whose RE are hydrolyzed to ROL by REH. Some of the incoming ROL is secreted into the bloodstream, bound to the retinol-binding protein (RBP) for peripheral distribution. The remainder is (i) oxidized by ROLDH, a reaction described as facilitated by CRBPI (C, see text for references), and RAL is next oxidized into RA by RALDH; (ii) degraded through the cytochrome P450 enzymes; (iii) transferred to HSC by unknown mechanisms, several of which are described as CRBPI dependent (A, see text for references). Once taken up by HSC, ROL is re-esterified as RE via ARAT which uses free ROL as substrate, and via LRAT which uses CRBPI-bound ROL as substrate (B, see text for references). Mobilization of RE stores from HSC requires hydrolysis by REH. The release of RE-derived ROL into the bloodstream is still unclear: ROL might be secreted from HSC bound to RBP, or might be first transferred back to hepatocytes (Blaner and Olson, 1994). Abbreviations: ARAT, acyl-CoA:retinol acyltransferase; LRAT, lecithin:retinol acyltransferase; P450, cytochrome P450; RA, retinoic acid; RAL, retinaldehyde; RALDH, retinaldehyde dehydrogenase; RBP, retinol-binding protein; RE, Retinyl esters; REH, retinyl ester hydrolase; ROL, retinol; ROLDH, retinol dehydrogenase. Question marks indicate still controversial hypotheses. Crosses indicate the pathways that might be impaired in CRBPI-null mice.

upon CRBPII; Ong *et al.*, 1988), as well as liver blood clearance are normal in our mutants.

Liver plays a pivotal role in maintaining ROL blood levels within a narrow range, by storing vitA in the case of dietary excess, and discharging vitA when dietary intake decreases. A model of ROL metabolism integrating the putative functions for CRBPI is depicted in Figure 7 (adapted from Napoli, 1993). Briefly, hepatocytes take up the chylomicrons, whose RE are hydrolyzed to ROL by REH. Some of the incoming ROL is transferred to HSC, in which it is esterified as RE via ARAT and LRAT. Mobilization of RE stores requires hydrolysis through REH activities, and its rate might be determined by the apo-/holo-CRBPI ratio. Free ROL should never accumulate inside cells, as the concentration of CRBPI always exceeds that of ROL (reviewed in Ross, 1993; Napoli, 1997).

The decreased capacity to store incoming ROL and to maintain RP stores in CRBP-I-null liver cannot be attributed to a loss or an aberrant differentiation of HSC, as shown in rats treated with xenobiotics (Azaïs-Braesco *et al.*, 1997). Indeed, mutant HSC appear to be morphologically normal and are capable of storing vitA, as evidenced by the presence of large lipid droplets in their cytoplasm upon oral administration of large doses of ROL (our unpublished data). The decreased level of RP in CRBPI-null liver may result from a reduced transfer of ROL from hepatocytes to HSC (A in Figure 7). A number of mechanisms have been proposed to account for this transfer, several of which involve CRBPI (Ottonello *et al.*, 1987; Noy and Blaner, 1991; Sundaram *et al.*, 1998). Furthermore, overexpression of CRBPI enhances uptake of ROL in transfected HL60 cells and HSC (Nilsson *et al.*, 1997). Decreased RP levels in CRBPI-null liver may also reflect an imbalance between accumulation and mobilization of RE in HSC (Troen *et al.*, 1994). Our data indicate a net hydrolysis of hepatic stores in CRBPI-null mice, as assessed by a decrease of RE half-life and higher amounts of [^{3}H]ROL in blood. This hydrolysis cannot be attributed to modified levels of enzymes synthesizing and hydrolyzing RE, but may reflect an impaired delivery of ROL to esterifying enzymes. Indeed LRAT (B in Figure 7), but not ARAT, requires CRBPI-bound ROL as a substrate for optimal activity *in vitro* (Yost *et al.*, 1988; Herr and Ong, 1992). The present study strongly suggests that CRBPI is also required, *in vivo*, for RE synthesis by LRAT in HSC. The RE content in CRBPI-null liver would then correspond to RE synthesis catalyzed by ARAT (and possibly LRAT) using free ROL as substrate. Interestingly, it was suggested that ARAT and LRAT may contribute equally to ROL esterification when the concentration of the substrate is higher than that of CRBPI, i.e. when most of the ROL is not bound to CRBPI (Randolph *et al.*, 1991). In any event, our results clearly indicate that CRBPI is required *in vivo* for efficient ROL esterification.

In spite of the defect in ROL esterification, the ROL serum level is maintained at normal values in CRBPI-null mutants. How this is achieved is unknown. We have not determined the daily rates of retinoid elimination in feces and urine. However, ROL catabolism is probably enhanced in the mutants, because CYP1A- and CYP2B-mediated activities are significantly increased.

CRBPI and retinoic acid homeostasis

In vitro studies (Ottonello *et al.*, 1993; reviewed in Napoli, 1997) and patterns of expression (Båvik *et al.*, 1997; Zhai *et al.*, 1997) have suggested that CRBPI could be essential for RA synthesis through ROLDH (see Figure 7). Accordingly, CRBPI deficiency should result in a decreased synthesis of RA. Our data rather suggest that the RA level could be increased, at least in liver of CRBPI-null newborns, as the expression of the RA-responsive RARβ2 gene is increased (see Figure 2D). Moreover, as (i) CRBPI-null mutant embryos and fetuses do not exhibit any abnormality characteristic of retinoic acid deficiency (reviewed in Kastner *et al.*, 1995) and (ii) mutant mice fed a VAD diet grow at a normal rate during 5 weeks [weight loss is an early symptom of RA deprivation (Anzano *et al.*, 1979)], it appears that RA homeostasis is not perturbed in CRBPI-null mice, at least during this period. Thus, CRBPI does not appear to be critically involved in ROL oxidation (C in Figure 7).

Once the vitA liver stores are exhausted, the CRBPI-null males exhibit the classical stigmas of the post-natal HVA syndrome described in rats, namely vision defects (Dowling and Wald, 1958), testicular degeneration and squamous keratinizing metaplasia (Wolbach and Howe, 1925; Beaver, 1961; Howell *et al.*, 1963). To date, this state of HVA has not been achieved with WT mouse strains. The morphological appearence of CRBPI-null testes after 14 weeks under the VAD diet represents a

clear phenocopy of the RARα-null phenotype (Lufkin *et al.*, 1993), indicating that the RARα-null mutation indeed reproduces a state of local vitA deprivation. The squamous keratinizing metaplasia observed in CRBPI-null mice fed the VAD diet (e.g. salivary glands, seminal vesicle, prostate, urethra and urinary bladder) are similar to those observed in old adult mice lacking RARγ (Lohnes *et al.*, 1993; our unpublished results) or described in VAD rats (Wolbach and Howe, 1925; Beaver, 1961). These data indicate that RA is necessary for the maintenance of these epithelia, its action being mediated by RARγ. It should be noted that keratinizing metaplasia of the respiratory tract, which represents a precocious feature of HVA in rat (Wolbach and Howe, 1925; Beaver, 1961), is never observed in CRBPI-null mice maintained on a VAD diet for a long time, nor in RAR-null mutants (Lohnes *et al.*, 1993; Lufkin *et al.*, 1993; Ghyselinck *et al.*, 1997; our unpublished results). This might reflect species-specific dependency on vitA for the maintenance of these epithelia.

Concluding remarks

The present report demonstrates that CRBPI deficiency has no apparent consequence on development and postnatal life, provided that vitA intake is high enough to compensate for the waste resulting from the decreased ROL storage and the increased RE store turnover. The World Health Organization listed more than 70 countries in which HVA could be considered as a problem of public health (MacLaren, 1986). All over the world, an estimated 124 million children are suffering from HVA, and therefore present higher risks of disease and death (Humphrey *et al.*, 1992). In the US and in European countries, HVA is not often encountered. However, dietary vitA intake may still be below the recommended allowance in a number of elderly people, premature newborns, some infected patients and pregnant women (Underwood *et al.*, 1970; Black *et al.*, 1988). These observations combined with the present results raise the question of the occurrence of mutations at the CRBPI locus in human beings, and of their consequences on health: absence of CRBPI might be without clinical effects in well-nourished populations, but might be highly deleterious in cases of dietary HVA.

Materials and methods

Homologous recombination

Genomic clones for the CRBPI locus were from a 129/Sv mouse DNA library. A 5.5 kb *Xba*I–*Xho*I fragment containing exons E1 and E2 was subcloned into pBSKII+ (Stratagene). A stop codon and an *Xma*I site were introduced into E2 at position 63 (Smith *et al.*, 1991), in which a NEO cassette was cloned. A TK cassette was inserted 3′ to the genomic DNA. If synthesized, the resulting protein would be truncated in the ligand-binding cavity, and therefore not be functional (Newcomer, 1995). The resulting plasmid was electroporated into D3 embryonic stem (ES) cells as described (Lufkin *et al.*, 1993). DNA from each G418 resistant clone was analyzed by Southern blotting. Once the mutant line had been established, genotyping was done by PCR. Amplification conditions and primer sequences are available upon request.

Mice and diets

Mice were on a mixed 129/Sv-C57BL/6 genetic background. The vitA-enriched diet contained 25 000 IU of RP/kg (UAR; Villemoisson sur Orge, France). The VAD diet was from UFAC (Vigny, France). Matings of mice were performed overnight. Noon of the day of a vaginal plug was taken as 0.5 day post-coitum (E0.5). Embryos were collected by Cesarean section and the yolk sacs were taken for genotyping. For retinoid analyses tissues were weighed and immediately frozen at –80°C.

RNA analysis

Transcript levels were analyzed by RNase protection assay using a standard protocol. Template for CRBPI riboprobe was obtained by subcloning a 204 nucleotide *Hin*cII–*Bpm*I fragment of the cDNA into pBSKII+. The CRBPII probe was transcribed from an *Eag*I linearized plasmid (pBSKII+) containing a 450 nucleotide PCR-amplified cDNA fragment which protected a fragment of 190 nucleotides. The histone H4 riboprobe, used as internal control, protected a 130 nucleotide fragment. Transcript levels were quantified using a BAS 2000 bioimaging analyzer (Fuji). The tRNA signal was used as the background value and data were normalized against the histone H4 values.

Protein analysis

Cytoplasmic proteins were analyzed according to Gaub *et al.* (1998). For immunohistochemistry, standard techniques were used (Wardlaw *et al.*, 1997) with polyclonal antibodies directed against CRBPI (MacDonald *et al.*, 1990; Gustafson *et al.*, 1993) or CRBPII (Schaefer *et al.*, 1989), and monoclonal antibodies specific for CRABPI and CRABPII (Gaub *et al.*, 1998). Immunodetections were visualized using protein A or anti-mouse immunoglobulins coupled to horseradish peroxidase, followed by chemiluminescence or DAB staining.

Histological and in situ hybridization analyses

Serial histological sections were stained with Groat's hematoxylin and Mallory's trichrome (Mark *et al.*, 1993). Liver samples were fixed in 3% glutaraldehyde (0.1 M sodium phosphate, pH 7.4), and 1 h in 1% phosphate buffered osmium tetroxide, dehydrated and embedded in araldite-epon. Semithin sections (2 μm thick) were stained with 1% toluidine blue in 5% sodium borate. Thin sections (65 nm) were contrasted with uranyl acetate and lead citrate, and examined using a Phillips EM208 electron microscope. *In situ* hybridizations were performed as described (Sapin *et al.*, 1997).

Analysis of retinoids

Tissue samples (300 mg) homogenized in 1 ml ethanol/water 50:50 (v/v) were extracted with hexane containing 0.1 mg/ml of butylated hydroxytoluene. Dried hexane phases were dissolved in ethanol. To monitor extraction yields, retinyl acetate was added to each sample. Analytical HPLC was carried out on a 3.9×300-mm C18 Novapack reverse phase column (Waters). Elution was for 45 min with a buffer containing 57.5% acetonitrile, 17.5% methanol, 0.5% acetic acid and 24.5% water, followed by a linear gradient to 100% methanol at 50 min and continuing with 100% methanol until completion of the run (constant flow rate, 1 ml/min). Absorbance was monitored at 325 nm. Compound identity and quantifications were deduced from retention times (as determined from pure retinoids, Sigma) and integrated peak areas, respectively. All values were normalized to 100% recovery, based on retinyl acetate recovery. Results are expressed as means ± SEM. Significance of differences was calculated by Student's *t* tests.

ROL turnover determination

Six-week-old mice, weaned at 4 weeks of age and averaging ~20 g, were randomly divided into six groups of eight each (four males and four females). Each mouse received orally 2.2×10^7 d.p.m. (10 μCi, specific activity 30 Ci/mmol) of [11,12-^{3}H(N)]retinol (NEN, Boston, MA) dissolved in 0.3 ml corn oil. Animals were killed at 6 h, 1, 2, 5, 10 and 20 days after dosing. Blood, liver, small intestine and kidney were collected. About 100 mg of tissue samples were incubated in 1 ml of BTS-450 tissue solubilizer (Beckman, Irvine, CA) for 4 h at 50°C. Samples were mixed with 9 ml of Ready Organic (Beckman) and radioactivity counted for 10 min in a Beckman LS6500 liquid scintillator.

Enzymatic activities

ARAT and LRAT activities were assayed on liver homogenates as described (Randolph *et al.*, 1991; Hanberg *et al.*, 1998). Phenylmethylsulfonyl fluoride (1.6 mM) was used as LRAT inhibitor. aREH activity was measured in sodium citrate buffer (pH 5) using RP (300 μM) incorporated into unilamellar liposomes as substrate (Mercier *et al.*, 1994). nREH was assayed in the presence of 150 mM 3-(3-cholamidopropyl dimethylammonio)-1 propanesulfonate dissolved in a Tris–maleate buffer (pH 7.2) using RP (1.5 mM) solubilized in Triton X-100 (0.2%) as substrate (Cooper and Olson, 1986). For CYP1A and 2B analysis, hepatic ethoxy- and pentoxy-resorufin-*O*-deethylase (EROD and PROD) activities were measured fluorimetrically in liver homogenates as described (Lubet

et al., 1985). Results are expressed as means ± SEM. Significance of differences was calculated by Student's *t* tests.

Electroretinography

Following a 24 h dark adaptation, animals were prepared under dim red illumination and anesthetized using ketamine (200 mg/kg) and xylazine (30 mg/kg). Pupils were dilated with a drop of 0.25% tropicamide. Electroretinogram (ERG) was recorded from the apex of the cornea using a cotton-wick connected to an Ag:AgCl electrode, and a stainless steel reference electrode placed subcutaneously on top of the head. ERG were elicited from one eye of each animal with a 50 ms bright white light flash (2.9 log cd/m^2) from a 150 W xenon lamp. Responses were amplified and filtered (low pass filter 0.1 Hz, high pass filter 1000 Hz) with a Universal Gould amplifier (Gould, Ballainvilliers, France).

Acknowledgements

We are grateful to M.P.Gaub, C.Egly, U.Eriksson and D.Ong for antibodies, and M.Petkovitch for the mouse CYP26 cDNA probe. We thank O.Wendling, S.Viville, D.Ong and J.Napoli for help, comments and discussions, and B.Bondeau, S.Bronner, B.Féret, M.C.Hummel, I.Tilly, B.Weber and the staff from the cell culture, microinjection, and animal facilities for technical assistance. This work was supported by funds from the Centre National de la Recherche Scientifique (CNRS), the Institut National de la Santé et de la Recherche Médicale (INSERM), the Hôpital Universitaire de Strasbourg, the Collège de France, the Association pour la Recherche sur le Cancer (ARC), Bristol-Myers Squibb and an EEC contract (FAIR-CT97-3220).

References

Abu-Abed,S.S., Beckett,B.R., Chiba,H., Chithalen,J.V., Jones,G., Metzger,D., Chambon,P. and Petkovich,M. (1998) Mouse P450RAI (CYP26) expression and retinoic acid-inducible retinoic acid metabolism in F9 cells are regulated by retinoic acid receptor γ and retinoid X receptor α. *J. Biol. Chem.*, **273**, 2409–2415.

Anzano,M.A., Lamb,A.J. and Olson,J.A. (1979) Growth, appetite, sequence of pathological signs and survival following the induction of rapid, synchronous vitamin A deficiency in the rat. *J. Nutr.*, **109**, 1419–1431.

Azaïs-Braesco,V., Hautekeete,M.L., Dodeman,I. and Geerts,A. (1997) Morphology of liver stellate cells and liver vitamin A content in 3,4,3′,4′-tetrachlorobiphenyl-treated rats. *J. Hepatol.*, **27**, 545–553.

Bashor,M.M., Toft,D.O. and Chytil,F. (1973) *In vitro* binding of retinol to rat-tissue components. *Proc. Natl Acad. Sci. USA*, **70**, 3483–3487.

Båvik,C., Ward,S.J. and Ong,D.E. (1997) Identification of a mechanism to localize generation of retinoic acid in rat embryos. *Mech. Dev.*, **69**, 155–167.

Beaver,D.L. (1961) Vitamin A deficiency in the germ-free rat. *Am. J. Pathol.*, **38**, 335–357.

Black,D.A., Heduan,E. and Mitchell,D. (1988) Hepatic stores of retinal and retinyl esters in elderly people. *Age Ageing*, **17**, 337–342.

Blaner,W.S. and Olson,J.A. (1994) Retinol and retinoic acid metabolism. In Sporn,M.B., Roberts,A.B. and Goodman,D.S. (eds), *Retinoids: Biology, Chemistry and Medicine*. Raven Press, New York, NY, pp. 229–255.

Blaner,W.S., Hendriks,F.J., Brouwer,A., deLeeuw,A.M., Knook,D.L. and Goodman,D.S. (1985) Retinoids, retinoid binding proteins, and retinyl palmitate hydrolase distributions in different types of rat liver cells. *J. Lipid Res.*, **26**, 1241–1251.

Blomhoff,R. *et al.* (1985) Hepatic retinol metabolism. Distribution of retinoids, enzymes, and binding proteins in isolated rat liver cells. *J. Biol. Chem.*, **260**, 13560–13565.

Blomhoff,R., Green,M.H., Green,J.B., Berg,T. and Norum,K.R. (1991) Vitamin A metabolism: new perspectives on absorption, transport, and storage. *Physiol. Rev.*, **71**, 951–990.

Boerman,M.H. and Napoli,J.L. (1991) Cholate-independent retinyl ester hydrolysis: stimulation by apo-cellular retinol binding protein. *J. Biol. Chem.*, **266**, 22273–22278.

Boerman,M.H. and Napoli,J.L. (1996) Cellular retinol-binding protein-supported retinoic acid synthesis. Relative roles of microsomes, and cytosol. *J. Biol. Chem.*, **271**, 5610–5616.

Carter-Dawson,L., Kuwabara,T., O'Brien,P.J. and Bieri,J.G. (1979) Structural and biochemical changes in vitamin A-deficient rat retinas. *Invest. Ophthalmol. Vis. Sci.*, **18**, 437–446.

Chambon,P. (1996) A decade of molecular biology of retinoic acid receptors. *FASEB J.*, **10**, 940–954.

Cooper,D.A. and Olson,J.A. (1986) Properties of liver retinyl ester hydrolase in young pigs. *Biochim. Biophys. Acta*, **884**, 251–258.

de Leeuw,A.M., Gaur,V.P., Saari,J.C. and Milam,A.H. (1990) Immunolocalization of cellular retinol-, retinaldehyde-, and retinoic acid-binding proteins in rat retina during pre-, and postnatal development. *J. Neurocytol.*, **19**, 253–264.

Dollé,P., Ruberte,E., Leroy,P., Morriss-Kay,G. and Chambon,P. (1990) Retinoic acid receptors, and cellular retinoid binding proteins. I. A systematic study of their differential pattern of transcription during mouse organogenesis. *Development*, **110**, 1133–1151.

Dowling,J.E. and Wald,G. (1958) Vitamin A deficiency and night blindness. *Proc. Natl Acad. Sci. USA*, **44**, 648–661.

Duester,G. (1996) Involvement of alcohol dehydrogenase, short-chain dehydrogenase/reductase, aldehyde dehydrogenase, and cytochrome P450 in the control of retinoid signaling by activation of retinoic acid synthesis. *Biochemistry*, **35**, 12221–12227.

Eriksson,U., Das,K., Busch,C., Nordlinder,H., Rask,L., Sundelin,J., Sallstrom,J. and Peterson,P.A. (1984) Cellular retinol binding protein. Quantitation, and distribution. *J. Biol. Chem.*, **259**, 13464–13470.

Gaub,M.P., Lutz,Y., Ghyselinck,N.B., Scheuer,I., Pfister,V., Chambon,P. and Rochette-Egly,C. (1998) New antibodies against cellular retinoic acid binding proteins CRABPI, and CRABPII. Evidence for a nuclear localization of CRABPs. *J. Histochem. Cytochem.*, **46**, 1103–1111.

Ghyselinck,N.B., Dupé,V., Dierich,A., Messaddeq,N., Garnier,J.M., Rochette-Egly,C., Chambon,P. and Mark,M. (1997) Role of the retinoic acid receptor beta (RARβ) during mouse development. *Int. J. Dev. Biol.*, **41**, 425–447.

Gustafson,A.L., Dencker,L. and Eriksson,U. (1993) Non-overlapping expression of CRBPI, and CRABPI during pattern formation of limb, and craniofacial structure in early mouse embryo. *Development*, **117**, 451–460.

Hanberg,A., Nilsson,C.B., Trossvik,C. and Håkansson,H. (1998) Effect of 2,3,7,8-tetrachloro dibenzo-*p*-dioxin on the lymphatic absorption of a single oral dose of [^{3}H]retinol and on intestinal retinol esterification in the rat. *J. Toxicol. Environ. Health*, **55**, 331–344.

Harrison,E.H. (1993) Enzymes catalyzing the hydrolysis of retinyl esters. *Biochim. Biophys. Acta*, **1170**, 99–108.

Herr,F.M. and Ong,D.E. (1992) Differential interaction of lecithin:retinol acyltransferase with cellular retinol binding proteins. *Biochemistry*, **31**, 6748–6755.

Howell,J.McC., Thompson,J.N. and Pitt,G.A.J. (1963) Histology of the lesions produced in the reproductive tract of animals fed a diet deficient in vitamin A alcohol but containing vitamin A acid. I. The male rat. *J. Reprod. Fertil.*, **5**, 159–167.

Humphrey,J.H., West,K.P. and Sommer,A. (1992) Vitamin A-deficiency and attributable mortality among under-5 years-olds. *Bull. World Health Organ.*, **70**, 225–232.

Johansson,S., Gustafson,A.L., Donovan,M., Romert,A., Eriksson,U. and Dencker,L. (1997) Retinoid binding proteins in mouse yolk sac, and chorio-allantoic placentas. *Anat. Embryol.*, **195**, 483–490.

Kastner,P., Mark,M. and Chambon,P. (1995) Nonsteroid nuclear receptors: what are genetic studies telling us about their role in real life? *Cell*, **83**, 859–869.

Kato,M., Sung,W.K., Kato,K. and Goodman,D.S. (1985) Immunohistochemical studies on the localization of cellular retinol binding protein in rat testis, and epididymis. *Biol. Reprod.*, **32**, 173–189.

Levin,M.S., Li,E., Ong,D.E. and Gordon,J.I. (1987) Comparison of the tissue-specific expression, and developmental regulation of two closely linked rodent genes encoding cytosolic retinol-binding proteins. *J. Biol. Chem.*, **262**, 7118–7124.

Lohnes,D., Kastner,P., Dierich,A., Mark,M., LeMeur,M. and Chambon,P. (1993) Function of retinoic acid receptor gamma in the mouse. *Cell*, **73**, 643–658.

Lubet,R.A., Nims,R.W., Mayer,R.T., Cameron,J.W. and Schechtman, L.M. (1985) Measurement of cytochrome P-450 dependent dealkylation of alkoxyphenoxazones in hepatic S9s, and hepatocyte homogenates: effects of dicumarol. *Mutat. Res.*, **142**, 127–131.

Lufkin,T., Lohnes,D., Mark,M., Dierich,A., Gorry,P., Gaub,M.P., LeMeur,M. and Chambon,P. (1993) High postnatal lethality and testis degeneration in retinoic acid receptor α mutant mice. *Proc. Natl Acad. Sci. USA*, **90**, 7225–7229.

MacDonald,P.N., Bok,D. and Ong,D.E. (1990) Localization of cellular retinol-binding protein and retinol-binding protein in cells comprising the blood-brain barrier of rat and human. *Proc. Natl Acad. Sci. USA*, **87**, 4265–4269.

MacLaren,D.S. (1986) Global occurrence of vitamin A-deficiency. In Bauerfeind,J.C. (ed.), *Vitamin A-Deficiency and its Control*. Academic Press Inc., London, UK, pp. 1–18.

Maden,M., Ong,D.E. and Chytil,F. (1990) Retinoid binding protein distribution in the developing mammalian nervous system. *Development*, **109**, 75–80.

Mark,M., Lufkin,T., Vonesch,J.L., Ruberte,E., Olivo,J.C., Dollé,P., Gorry,P., Lumsden,A. and Chambon,P. (1993) Two rhombomeres are altered in Hoxa-1 mutant mice. *Development*, **119**, 319–338.

Mercier,M., Forget,A., Grolier,P. and Azaïs-Braesco,V. (1994) Hydrolysis of retinyl esters in rat liver. Description of a lysosomal activity. *Biochim. Biophys. Acta*, **1212**, 176–182.

Nakshatri,H. and Chambon,P. (1994) The directly repeated RG(G/T)TCA motifs of the rat and mouse cellular retinol-binding protein II genes are promiscuous binding sites for RAR, RXR, HNF-4, and ARP-1 homo- and heterodimers. *J. Biol. Chem.*, **269**, 890–902.

Napoli,J.L. (1993) Biosynthesis and metabolism of retinoic acid: roles of CRBP and CRABP in retinoic acid homeostasis. *J. Nutr.*, **123**, 362–366.

Napoli,J.L. (1997) Retinoid binding proteins redirect retinoid metabolism: biosynthesis and metabolism of retinoic acid. *Semin. Cell Dev. Biol.*, **8**, 403–415.

Newcomer,M.E. (1995) Retinoid binding proteins: structural determinants important for function. *FASEB J.*, **9**, 229–239.

Nilsson,M.H., Spurr,N.K., Lundvall,J., Rask,L. and Peterson,P.A. (1988) Human cellular retinol binding protein gene organization, and chromosomal location. *Eur. J. Biochem.*, **173**, 35–44.

Nilsson,A., Troen,G., Petersen,L.B., Reppe,S., Norum,K.R. and Blomhoff,R. (1997) Retinyl ester strorage is altered in liver stellate cells and in HL60 cells transfected with cellular retinol-binding protein type I. *Int. J. Biochem. Cell Biol.*, **29**, 381–389.

Noy,N. and Blaner,W.S. (1991) Interactions of retinol with binding proteins: studies with rat cellular retinol-binding protein and rat retinol-binding protein. *Biochemistry*, **30**, 6380–6386.

Ong,D.E. (1994) Cellular transport, and metabolism of vitamin A: role of the cellular retinoid-binding proteins. *Nutr. Rev.*, **52**, 24–31.

Ong,D.E., McDonald,P.N. and Gubitosi,M. (1988) Esterification of retinol in rat liver. Possible participation by cellular retinol binding protein, and cellular retinol binding protein II. *J. Biol. Chem.*, **263**, 5789–5796.

Ottonello,S., Petruccc,S. and Maraini,G. (1987) Vitamin A uptake from retinol-binding protein in a cell-free system from pigment epithelial cells of bovine retina. *J. Biol. Chem.*, **262**, 3975–3981.

Ottonello,S., Scita,G., Mantovani,G., Cavazzini,D. and Rossi,G.L. (1993) Retinol bound to cellular retinol binding protein is a substrate for cytosolic retinoic acid synthesis. *J. Biol. Chem.*, **268**, 27133–27142.

Peterson,P.A., Rask,L., Ostberg,L., Andersson,L., Kamwendo,F. and Pertoft,H. (1973) Studies on the transport and cellular distribution of vitamin A in normal and vitamin A-deficient rats with special reference to the vitamin A-binding plasma protein. *J. Biol. Chem.*, **248**, 4009–4022.

Porter,S.B., Ong,D.E., Chytil,F. and Orgebin-Crist,M.C. (1985) Localization of cellular retinol binding protein, and cellular retinoic acid binding protein in the rat testis and epididymis. *J. Androl.*, **6**, 197–212.

Randolph,R.K., Winkler,K.E. and Ross,A.C. (1991) Fatty acyl CoA-dependent, and CoA-independent retinol esterification by rat liver, and lactating mammary gland microsomes. *Arch. Biochem. Biophys.*, **288**, 500–508.

Ross,A.C. (1993) Cellular metabolism, and activation of retinoids: roles of cellular retinoid-binding proteins. *FASEB J.*, **7**, 317–327.

Ruberte,E., Dollé,P., Chambon,P. and Morriss-Kay,G. (1991) Retinoic acid receptors, and cellular retinoid binding proteins. II. Their differential pattern of transcription during early morphogenesis in mouse embryos. *Development*, **111**, 45–60.

Sapin,V., Ward,S.J., Bronner,S., Chambon,P. and Dollé,P. (1997) Differential expression of transcripts encoding retinoid binding proteins, and retinoic acid receptors during placentation of the mouse. *Dev. Dyn.*, **208**, 199–210.

Schaefer,W.H., Kakkad,B., Crow,J.A., Blair,I.A. and Ong,D.E. (1989) Purification, primary structure characterization, and cellular distribution of two forms of cellular retinol-binding protein, type II from adult rat small intestine. *J. Biol. Chem.*, **264**, 4212–4221.

Shenai,J.P. and Chytil,F. (1990) Vitamin A storage in lungs during perinatal development in the rat. *Biol. Neonate*, **57**, 126–132.

Smith,W.C., Nakshatri,H., Leroy,P., Rees,J. and Chambon,P. (1991) A retinoic acid response element is present in the mouse cellular retinol binding protein I (mCRBPI) promoter. *EMBO J.*, **10**, 2223–2230.

Sucov,H.M., Murakami,K.K. and Evans,R.M. (1990) Characterization of an autoregulated response element in the mouse retinoic acid receptor type beta gene. *Proc. Natl Acad. Sci. USA*, **87**, 5392–5396.

Sundaram,M., Sivaprasadarao,A., DeSousa,M.M. and Findlay,J.B. (1998) The transfer of retinol from serum retinol-binding protein to cellular retinol-binding protein is mediated by a membrane receptor. *J. Biol. Chem.*, **273**, 3336–3342.

Troen,G., Nilsson,A., Norum,K.R. and Blomhoff,R. (1994) Characterization of liver stellate cell retinyl ester storage. *Biochem. J.*, **300**, 793–798.

Troen,G., Eskild,W., Fromm,S.H., Reppe,S., Nilsson,A., Norum,K.R. and Blomhoff,R. (1996) Retinyl ester storage is normal in transgenic mice with enhanced expression of cellular retinol-binding protein type I. *J. Nutr.*, **126**, 2709–2719.

Underwood,B.A., Siegel,H., Weisell,R.C. and Dolinski,M. (1970) Liver stores of vitamin A in a normal population dying suddenly or rapidly from unnatural causes in New York city. *Am. J. Clin. Nutr.*, **23**, 1037–1042.

Wake,K. (1980) Perisinusoidal stellate cells (fat-storing cells, interstitial cells, lipocytes), their related structure in, and around the liver sinusoids, and vitamin A-storing cells in extrahepatic organs. *Int. Rev. Cytol.*, **66**, 303–353.

Wardlaw,S.A., Bucco,R.A., Zheng,W.L. and Ong,D.E. (1997) Variable expression of cellular retinol, and cellular retinoic acid binding proteins in the rat uterus, and ovary during the estrous cycle. *Biol. Reprod.*, **56**, 125–132.

Wolbach,S.B. and Howe,P.R. (1925) Tissue changes following deprivation of fat-soluble A vitamin. *J. Exp. Med.*, **42**, 753–777.

Yost,R.W., Harrison,E.H. and Ross,A.C. (1988) Esterification by rat liver microsomes of retinol bound to cellular retinol binding protein. *J. Biol. Chem.*, **163**, 18693–18701.

Zetterström,R.H., Simon,A., Giacobini,M.M., Eriksson,U. and Olson,L. (1994) Localization of cellular retinoid binding proteins suggests specific roles for retinoids in the adult central nervous system. *Neuroscience*, **62**, 899–918.

Zhai,Y., Higgins,D. and Napoli,J.L. (1997) Coexpression of the mRNAs encoding retinol dehydrogenase isozymes and cellular retinol-binding protein. *J. Cell. Physiol.*, **17**, 36–43.

Received June 2, 1999; revised and accepted July 22, 1999